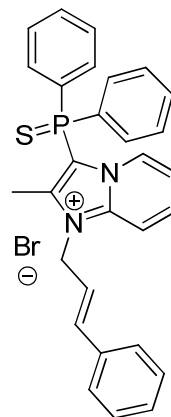


Probe Report

Title: Identification of Novel Small Molecule Antagonists of the Neuropeptide-S Receptor
 Authors: Markus Heilig
 Assigned Assay Grant #: X01-DA026210-01
 Screening Center Name & PI: NCGC & Christopher P. Austin
 Chemistry Center Name & PI: NCGC & Christopher P. Austin
 Assay Submitter & Institution: Markus Heilig, National Institute on Alcohol Abuse and Alcoholism
 PubChem Summary Bioassay Identifier (AID): 1461

Probe Structure & Characteristics:

PubChem CID: 46930969
 Internal ID: NCGC00185684-01
 IUPAC Name: 1-Cinnamyl-3-(diphenylphosphorothioyl)-2-methylimidazo[1,2-a]pyridin-1-ium bromide
 Chemical Formula: $C_{29}H_{26}BrN_2PS$
 Exact Mass: 544.0738 (465.1549 for cation)



ML154

CID/ML#	Target Name	IC50/EC50 (nM) [SID, AID]	Anti-target Name(s)	IC50/EC50 (μM) [SID, AID]	Fold Selective	Secondary Assay(s) Name: IC50/EC50 [SID, AID] (nM)
46930969/ ML154	NPSR	1nM (Ca2+) [87796314, 2567] 45nM (cAMP) [87796314, 2568]	V1B Vasopressin Receptor (27% Identity with NPSR)	>57μM [87796314, 2570]	>100-fold	[125I]Y10-hNPS displacement: 1.0 nM [87796314, 2566]

Recommendations for scientific use of the probe:

This probe report is a revised version that has been updated to include additional data, address points raised during review, and conform to the requirements of the latest MLPCN probe report template.

There is a clear need to discover novel small molecule antagonists of the Neuropeptide S Receptor (NPSR) to help probe NPS/NPSR pharmacology and to validate the importance of this neurocircuitry in animal models. SHA68, a compound disclosed by Takeda Pharmaceutical

Company, shows only 50% efficacy in an *in vivo* hyperlocomotion mouse model. An additional chemotype disclosed by Merck shows *ex vivo* receptor occupancy in discrete regions of the rat brain after intraperitoneal (IP) dosing. However, no small molecule has yet demonstrated robust *in vivo* efficacy in multiple animal models. The present report discloses the discovery and characterization of a potent NPSR antagonist having an imidazo-pyridinium molecular core and an unusual, yet stable phosphorothioyl species. Synthetic methodology, SAR for both Gq and Gs coupled functional pathways and activity of our most potent compound in a NPS displacement assay are presented. The probe molecule is the most potent compound yet reported and has promising microsomal stability compared to other lead NPSR antagonists disclosed in the literature. *In vivo* rodent pharmacokinetic experiments show that a 10 mpk dose administered IP may provide sufficient exposure in brain to see functional antagonism for many hours. The probe completely antagonizes NPS activation of the NPS/NPSR neurocircuitry in a food intake rat model using intracerebroventricular (icv) administration.

This potent probe molecule can be used as a tool molecule by biologists interested in understanding NPS/NPSR pharmacology and the role of NPSR antagonism in sleep, anxiety, food intake, and addiction.



1 Introduction

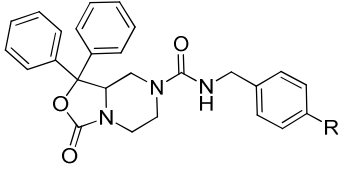
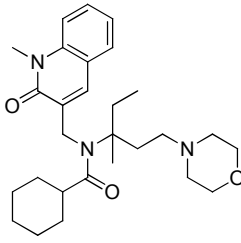
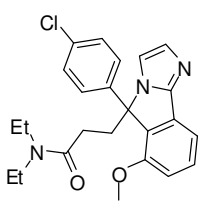
The last decade has witnessed an incremental understanding of the neuropeptidic circuitry and its crucial role in controlling many physiological processes of the central nervous system.¹ A great deal of attention has focused on neuropeptide S (NPS) and its receptor, the neuropeptide S receptor (NPSR). NPSR is a G-protein coupled receptor that was first described by Sato and co workers in 2004.² Subsequently it was deorphanized by Xu, who described the structure of NPS as a 20-amino acid endogenous ligand which binds to NPSR.³ Later on, the same group also detailed the distribution and expression of NPS precursor mRNA and NPSR mRNA in various regions of the brain.⁴ Additionally, it was shown that central administration of NPS promotes hyperlocomotion and wakefulness in various rodent models, implicating the importance of this circuitry in the control of sleep, stress, anxiety and arousal.⁵ Additionally, two polymorphisms of NPSR, Ile107 from Asn107 and a C-terminal splice variant, were linked to asthma.⁶ Moreover, Reinscheid et al. detailed the NPS/NPSR pharmacology via stable cell lines expressing NPSR and these variants,⁷ characterizing a binding assay which monitored the displacement of radiolabeled 125I-NPS ligand by the cognate NPS ligand. They also described three separate functional assays which increased calcium mobilization, cAMP formation, and p42/p44 MAPK phosphorylation in a dose-dependent manner on addition of NPS. This work suggested that the receptor is coupled to signaling through the Gq, Gs and MAPK pathways, and also shows that the I107N NPSR variant displayed an increased functional potency in all these assays but not in binding affinity. Recently, the possible importance of the extracellular loop one, where this SNP is located, has been highlighted in the biogenesis and function of NPSR.⁸

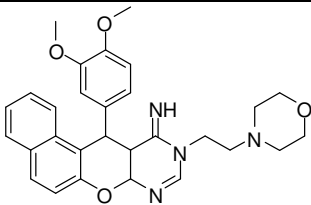
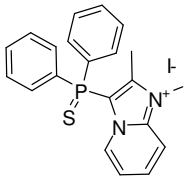
In vivo work in rodents has implicated the NPS/NPSR signaling role in controlling oxidative stress⁹ and the intake of food.¹⁰ Recently, our collaborator Roberto Ciccocioppo and co-workers demonstrated that antagonism of this pathway also holds promise as a therapy for prevention of relapse to alcoholism.¹¹ They reported that administration of NPS in the lateral hypothalamus of the rat brain resulted in a significant increase in cue-induced alcohol seeking behavior in an alcohol relapse rat model. This effect was reduced by the selective oxerlin receptor antagonist SB-334867, indicating the presence of a strong link between the Hcrt-1/Ox-A and the NPS signaling pathways. Similar *in vivo* work has also implicated this circuitry's relevance towards addition to cocaine and morphine.¹²

Guerrini and co-workers have published much work on generating and analyzing various analogs around the 20 amino acid sequence SFRNGVGTGMKTSFQRAKS, in NPS which is highly conserved amongst tetrapods.¹³ This work has led to the discovery of potent peptide agonists and antagonists of NPSR. It has also identified the essential amino acids in the

neuropeptide responsible for its pharmacology.¹⁴ Small molecules also play an invaluable role for studying such novel signaling systems. They often hold high potential with respect to drug development and therapeutic intervention in disease control. In this regard two molecules, SHA 66 (**1a**) and SHA 68 (**1b**), disclosed by Takeda Pharmaceuticals,¹⁵ have been characterized pharmacologically as potent inhibitors on the NPS/NPSR signaling pathway (Table 1). A 50 mpk intraperitoneal (IP) dose of SHA68 was also able to reduce NPS-induced hyperlocomotion in a 90 minute rat model by only about 50%.¹⁶ This was surprising, because PK studies reported the compound had exposure in the brain that was well beyond its *in vitro* IC₅₀ (~6 μ M at 15 min, ~2 μ M @ 2 h). It can be speculated that the weak *in vivo* activity might be related to its GPCR selectivity profile or the fast clearance associated with this compound. Recently, potent inhibitors from two separate chemical series (**2a** and **2b**) were disclosed by Merck.^{17, 18} The best compound from a quinolinone class (**2a**) demonstrated high *ex vivo* occupancy of NPSR after a 30 mpk IP dose in discrete regions of the rat brain. However, none of these compounds have been shown to demonstrate *in vivo* efficacy in animal models of disease. Therefore, there is still an unmet need to develop novel small molecule antagonists which can be used as tools to understand and demonstrate the importance of the NPSR neurobiology in diseased states. Recently, our efforts at the NCGC have resulted in the disclosure of a naphtho pyrano pyrimidine probe (**3**) where structural changes in the same chemical series led to selective modulators of either the Gq or Gs pathway.¹⁹ Herein we disclose the discovery of another novel chemotype (**4**) and its SAR and optimization into a potent, functional antagonist of the NPSR.

Table 1: Activity of hit compound along with previously disclosed NPS antagonists

Structure	R	Cpd#	¹²⁵ I-hNPS displacement IC ₅₀ nM	Ca ²⁺ IC ₅₀ nM	cAMP IC ₅₀ nM	PubChem CID
	H	1a	26	ND	ND	11177829
	F	1b	5.9	139	1940	11374217
		2a	6.5	1	55	44156964
		2b	43	ND	ND	46203026

	3	190	1585	1259	3719993
	4	84	220	1120	16196125

2 Materials and Methods

2.1 Assays

PubChem AID	Type	Target	Conc. Range	Samples Tested	Notes
1461	Primary qHTS	NPSR1	46.1 μ M – 3 nM	221,370	cAMP signaling
1491	Confirmatory	NPSR1	47.8 μ M – 0.1 nM	259	cAMP signaling
1489	Secondary	NPSR1	50.8 μ M – 0.3 nM	213	Ca++ signaling
1492	Secondary	CHRM1	50.8 μ M – 0.3 nM	85	Ca++ signaling
1493	Secondary	NPSR1	45 μ M – 0.1 nM	16	NPS displacement
2568	Confirmatory	NPSR1	47.8 μ M – 0.1 nM	186	cAMP signaling
2567	Secondary	NPSR1	50.8 μ M – 0.3 nM	186	Ca++ signaling
2570	Secondary	AVPR1B	28.7 μ M – 0.1 nM	88	Ca++ signaling
2566	Secondary	NPSR1	45 μ M – 0.1 nM	20	NPS displacement
434936	Confirmatory	NPSR1	47.8 μ M – 0.1 nM	77	cAMP signaling
434931	Secondary	NPSR1	50.8 μ M – 0.3 nM	77	Ca++ signaling
1464	Summary	NPSR			

Table 2: Data deposited into PubChem describing initial screening and confirmation of NPSR antagonists.

In general, compounds active in the initial cAMP-based functional screen, were confirmed in that screen and also a calcium signaling-based assay of NPSR activity as an orthogonal measure of activity. Compounds were initially counterscreened against a muscarinic M1 receptor (CHRM1) calcium signaling-based assay, but later hits were counterscreened against the vasopressin receptor (AVPR1B) owing to its stronger sequence similarity to NPSR (it is the

most homologous G-protein coupled receptor to NPSR). Finally, select compounds were characterized for displacement of NPS from NPSR to verify orthosteric binding.

qHTS Assay for Antagonists of the Neuropeptide S Receptor: cAMP Signal Transduction [AIDs: 1461, 1491, 2568, 434936]

Assay Description

It is known that NPS stimulates the cAMP signaling pathway and increases the cAMP level in cells expressing NPS receptor. This change in intracellular cAMP level can be detected by a cAMP HTRF assay (Fig 2), which is based on TR-FRET (time resolved fluorescence resonance energy transfer) between a cAMP-specific antibody labeled with europium (Eu) cryptate (Ab-cAMP-Eu), and a cAMP analog conjugated to the fluorescent dye d2 (cAMP-d2). Light pulse at 320 nm excites the europium of Ab-cAMP-Eu and the energy emitted is transferred to the cAMP-d2 bound to the antibody, generating a TR-FRET signal at 665 nm. Residual energy from the Eu-cryptate will produce a light at 620 nm. The native unlabeled cAMP from cell lysates competes with the cAMP-d2 for Ab-cAMP-Eu binding and reversely reduces the emission signal of cAMP-d2 by interrupting FRET between the two labeled molecules. Both emission signals from the FRET donor (620 nm) and the acceptor (665 nm) can be measured by a plate reader. Expression of result in fluorescence ratio (665 nm/620 nm) helps to normalize differences due to cell density and reagent dispensing.

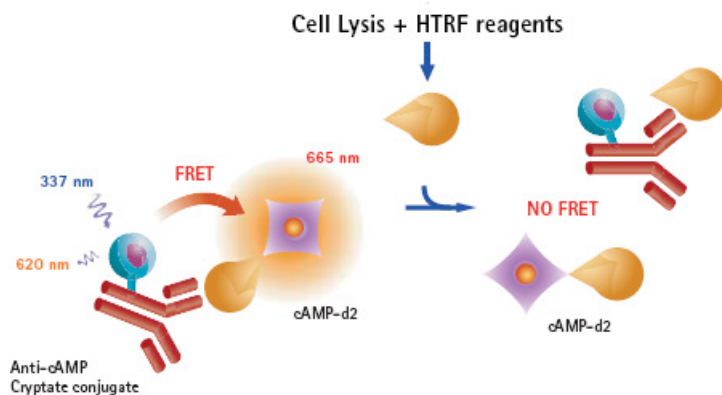


Figure 1: Schematic illustration of the assay principle of the HTRF cAMP assay.

Assay Protocol

All of the reagents used for the NPSR cAMP assay and their resources are listed in Table 3. A schematic illustration of the assay principle is shown in Figure 1. The assay protocol is described below, and in Table 4.

Table 3: Reagents and resources for the HTRF cAMP assay

Reagents	Resources	Catalog Number
HTRF cAMP <i>dynamic</i> 2 kit	Cisbio	62AM4PEJ
Ro 20-1724	Sigma-Aldrich	B8279
NPS peptide	Provided by PI	
F12 Nutrient Mixture (Ham)	Invitrogen	11765
Fetal Bovine Serum	Invitrogen	10091
Penicillin-Streptomycin	Invitrogen	15140
Geneticin	Invitrogen	10131
Tween-20	Sigma-Aldrich	P9416

A Chinese hamster ovary (CHO) cell line stably expressing the NPSR was generated in Dr. Heilig's lab. The cells were maintained in F12 medium containing 10 % FBS, 100 units/ml Penicillin, 100 µg/ml Streptomycin, and 200 µg/ml Geneticin at 37 °C, 5% CO₂.

Suspended CHO-NPSR cells were seeded into 1536-well tissue culture-treated white plates at a density of 1800 cells/well in 4 µl media without Geneticin and incubated at 37 °C, 5 % CO₂ for overnight. After 1µl of stimulation buffer (1X PBS buffer, 0.1% BSA, 0.05% Tween-20, 500µM Ro 20-1724, EC80 of NPS) was added to each well, cells were incubated at 37 °C, 5 % CO₂ for 30 min. 1.25 µl of d2 conjugated cAMP and 1 µl cryptate conjugated anti-cAMP antibody were then added. D2 conjugated cAMP and cryptate conjugated anti-cAMP antibody were both prepared in cell lysis buffer according to the manufacturer's instruction. After 30 minutes, plates were then read in Viewlux plate reader (Perkin Elmer) using the TRF detection mode optimized for HTRF.

Table 4: cAMP assay protocol for the CHO-NPSR cells in 1536-well plate format

Step	Parameter	Value	Description
1	Cells	4µl	1800 cells/well
2	Culture	18-30 hr	37°C, 5% CO ₂
3	Compound	23 nl	Library Compounds in 0.128 to 10 mM titration series or control
4	Reagent	1 µl	Stimulation buffer

5	Incubation	30 min	37°C, 5% CO ₂
6	Reagent	1.25 µl	D2 conjugated cAMP
7	Reagent	1.25 µl	Cryptate conjugated anti-cAMP antibody
8	Incubation	120 min	Room temperature
9	Detector	Ex 320, Em 615/665	Viewlux plate reader

qHTS Assay for Antagonists of the Neuropeptide S Receptor: Calcium Mobilization [AID: 1489, 2567, 434931]

Assay Description

The fluorescent calcium dye Fluo-4 AM has been widely used in GPCR studies to visualize and measure changes in intracellular calcium. It is able to enter the cell by passive diffusion and is de-esterified by endogenous esterases in the cytosol that are not fluorescent. The dye becomes fluorescent upon binding of calcium, resulting in fluorescent signals proportional to the cytosol free calcium concentration that is dramatically increased by the stimulation of certain GPCRs. Because intracellular calcium responses are transient with a fast kinetic (a half-life in the range of seconds to minutes), its detection requires special instruments that combine both the automated reagent dispenser and the kinetic fluorescence reader. A FDSS-7000 system (FDSS, Hamamatsu, Hamamatsu City, Japan) was used at NCGC to measure the intracellular calcium changes in response to agonist stimulation on GPCRs.

Table 5: Reagents and resources for the calcium mobilization assay

Reagents	Resources	Catalog Number
High Performance PBX Calcium Assay Kit	BD, Rockville, MD	644209
F12 Nutrient Mixture (Ham)	Invitrogen	11765
Fetal Bovine Serum	Invitrogen	10091
Penicillin-Streptomycin	Invitrogen	15140
Geneticin	Invitrogen	10131
Tween-20	Sigma-Aldrich	P9416
Ro 20-1724	Sigma-Aldrich	B8279
NPS peptide	Provided by PI	

Assay Protocol

All of the reagents used for this assay and their resources are listed in Table 5. The assay protocol is described below, and in table 6.

The CHO-NPSR cell line used in the cAMP assay was also used in this calcium mobilization assay. The suspended cells were plated at 3 μ l/well with 2000 cells in the black, tissue culture treated, clear bottom 1536-well plates. After overnight incubation at 37 $^{\circ}$ C, 5% CO₂, 3 μ l of the calcium dye (no wash High Performance PBX Calcium Assay Kit, BD Biosciences) was loaded to each well and the plates were incubated at 37 $^{\circ}$ C, 5 % CO₂ for 1 hour followed by 10-min incubation with 23 nl compound prepared in DMSO solution. The assay plates were then placed onto the FDSS-7000 kinetic fluorescence plate reader for measuring the changes of intracellular free calcium. The basal fluorescence signal was recorded for 6 sec at 1 Hz followed by an addition of 1 μ l of NPS stimulation buffer (1X PBS buffer, 0.1% BSA, 0.05% Tween-20, 500 μ M Ro 20-1724, EC80 of NPS) and 4-minute continuous recording at 1 Hz.

Table 6: Calcium mobilization assay protocol for the CHO-NPSR cells in 1536-well plate format

Step	Parameter	Value	Description
1	Cells	3 μ l	2000 cells/well
2	Culture	18-30 hr	37 $^{\circ}$ C, 5% CO ₂
3	Reagent	3 μ l	Calcium dye
4	Incubation	1 hr	37 $^{\circ}$ C, 5% CO ₂
5	Compound	23 nl	Library Compounds in 0.128 to 10 mM titration series or control
6	Incubation	10 min	37 $^{\circ}$ C, 5% CO ₂
8	Reagent	1 μ l	Stimulation buffer
9	Detector	Ex 480 nm, Em 520-560 nm	FDSS-7000 kinetic fluorescence plate reader Fluo-4 filter set

Counterscreen for Antagonists of the Neuropeptide S Receptor: Muscarinic Acetylcholine M1 Receptor Antagonism [AID: 1492]

Assay Description

Muscarinic acetylcholine M1 receptor is a G protein-coupled receptor found in the plasma membranes of certain neurons and other cells. Because this receptor is coupled to the same G proteins as NPSR, it provides a good counterscreen for compounds that antagonize signal

transduction through receptor-independent mechanisms (such as direct modulators of cellular cAMP levels).

Table 7: Reagents and resources for the calcium mobilization assay

Reagents	Resources	Catalog Number
High Performance PBX Calcium Assay Kit	BD, Rockville, MD	644209
F12 Nutrient Mixture (Ham)	Invitrogen	11765
Fetal Bovine Serum	Invitrogen	10091
Penicillin-Streptomycin	Invitrogen	15140
Geneticin	Invitrogen	10131
Carbachol	Sigma-Aldrich	C4382

Assay Protocol

All of the reagents used for this assay and their resources are listed in Table 7. The assay protocol is described below, and in Table 8.

A Chinese hamster ovary (CHO) cell line stably expressing muscarinic acetylcholine M1 receptor (CHO-M1) was obtained from ATCC and maintained in F-12 Kaighn's media (Invitrogen, Carlsbad, CA, 21127) supplemented with 10 % FBS, 100 units/ml penicillin, 100 ug/ml streptomycin and 250 ug/ml geneticin at 37C, 5% CO₂ in a humidified atmosphere. Before the assay, aliquots of cells were frozen and stored at -135C. The assay was performed on a FDSS-7000 kinetic plate reader in 1536-well format. The maximums of kinetic fluorescence responses were converted into text files using the instrument's software data export utility. Data for antagonist response were normalized to the controls for basal activity (DMSO only) and 100% inhibition. AC₅₀ values were determined from concentration-response data modeled with the standard Hill equation.

Frozen CHO-M1 cells were thawed, washed once with fresh media and resuspended in F-12 Kaighn's media supplemented with 10 % FBS, 100 units/ml penicillin and 100 ug/ml streptomycin. Cells were plated at 3 µl/well (1200 cells) into black, clear-bottom, tissue-culture treated 1536-well plates, and then cultured at 37C, 5 % CO₂ for 16 to 30 hours. 3 µl of calcium dye (from High Performance PBX Calcium Assay Kit, BD Biosciences) was added. The calcium dye was prepared according to the manufactory's instruction. Plates were incubated at 37C, 5 % CO₂ for 1 hour. Add 23 nl/well of compound in DMSO solution was added. The final titration for each compound was between 0.6 nM and 46 uM. Plates were then loaded onto the FDSS-7000. The following steps were performed on the FDSS-7000. (1) Record fluorescent

background (Ex 480 nm, Em 520-560 nm) for 10 s. (2) Add 2 μ l of stimulation buffer (1X HBSS buffer, 0.1% BSA, 60 nM carbachol). (3) Record antagonist response (Ex 480 nm, Em 520-560 nm) for 180 s.

Table 8: Calcium mobilization assay protocol for the CHO-M1 cells in 1536-well plate format

Step	Parameter	Value	Description
1	Cells	3 μ l	1200 cells/well
2	Culture	16-30 hr	37°C, 5% CO ₂
3	Reagent	3 μ l	Calcium dye
4	Incubation	1 hr	37°C, 5% CO ₂
5	Compound	23 nl	Library Compounds in 0.128 to 10 mM titration series or control
6	Incubation	10 min	37°C, 5% CO ₂
8	Reagent	2 μ l	Stimulation buffer
9	Detector	Ex 480 nm, Em 520-560 nm	FDSS-7000 kinetic fluorescence plate reader Fluo-4 filter set

qHTS Assay for Antagonists of the Neuropeptide S Receptor: Radioactive Ligand Displacement [AIDs: 1493, 2566]

Assay Description

Select samples was tested in a direct ligand binding assay, measuring [¹²⁵I] Y¹⁰-hNPS displacement as previously described²⁰.

Assay Protocol

All of the reagents used for this assay and their resources are listed in Table 9. The assay was carried out as described²⁰ with minor modification. Y10-NPS labeled with 125I was bought from NEN Perkin Elmer (Boston, MA). CHO cells stably expressing human NPSR were seeded into 24-well plates and cultured until reaching 90-95% confluency. Cells were washed with 1ml PBS once, and then incubated with radioligand with or without compounds or in DMEM medium containing 0.1% bovine serum albumin at 20C for 1.5 hr. Increasing concentrations of compounds or unlabeled human NPS were used to compete with 0.15 nM [125I] Y10-NPS. Nonspecific binding was determined in the presence of 1 μ M unlabeled human NPS. Cells were washed twice with cold PBS and lysed with 1 N NaOH. Bound radioactivity was counted in a liquid scintillation counter.

Table 9: Reagents and resources for the radioactive ligand binding assay

Reagents	Resources	Catalog Number
F12 Nutrient Mixture (Ham)	Invitrogen	11765
Fetal Bovine Serum	Invitrogen	10091
Penicillin-Streptomycin	Invitrogen	15140
Geneticin	Invitrogen	10131
[¹²⁵ I] Y ¹⁰ -hNPS	NEN Perkin Elmer	

2.2 Probe Chemical Characterization

Structural Verification of the Probe

1-Cinnamyl-3-(diphenylphosphorothioyl)-2-methylimidazo[1,2-a]pyridin-1-ium bromide (CID 46930969) ¹H NMR (400 MHz, DMSO-*d*₆) δ ppm 1.75 (d, *J*=1.4 Hz, 3 H), 5.28 (m, 2 H), 6.43 (m, 1 H), 6.86 (d, *J*=16.0 Hz, 1 H), 7.32 (m, 3 H), 7.44 (m, 2H), 7.59 (td, *J*=7.1, 1.3 Hz, 1 H), 7.68 (m, 4 H), 7.78 (m, 2 H), 7.91 (m, 4 H), 8.20 (ddd, *J*=9.2, 7.2, 1.2 Hz, 1 H), 8.48 (m, 1 H), 8.70 (m, 1 H).

HRMS: *m/z* (*M*⁺) = 465.1553 (Calculated for C₂₉H₂₆N₂PS⁺ = 465.1549).

LC/MS (Agilent system) Retention time *t*₁ (long) = 5.456 min

Purity: UV₂₂₀ > 99%, UV₂₅₄ > 99%; MS *m/z* 291.1 (*M*+*H*);

Column: Phenomenex Luna C18 (3 micron, 3 x 75 mm).

Run time: 8 min (long)

Gradient: 4% to 100% Acetonitrile in water over 7 min

Mobile phase: Acetonitrile (0.025 % TFA), water (0.05 % TFA).

Flow rate: 1 mL/min

Temperature: 50 °C

UV wavelength: 220 nm, 254 nm

Summary of Probe Properties

PubChem CID: 46930969, SID: 87796314, ML154

IUPAC Name: 1-Cinnamyl-3-(diphenylphosphorothioyl)-2-methylimidazo[1,2-a]pyridin-1-ium bromide

Canonical SMILES:

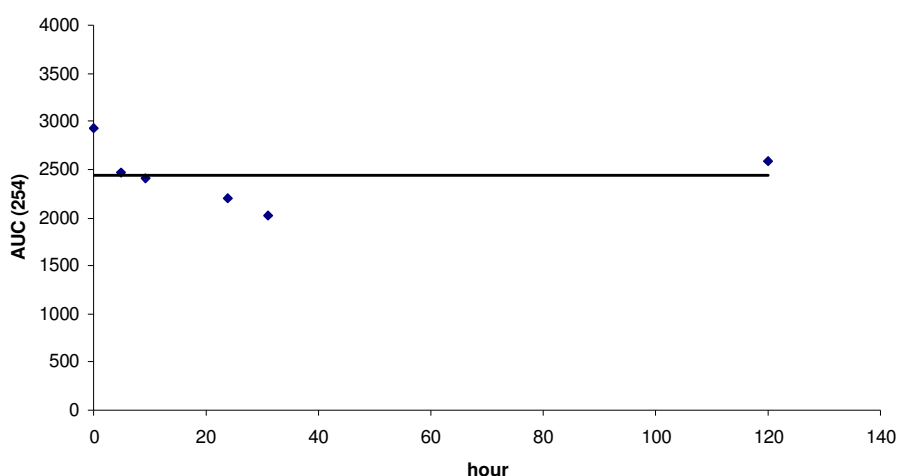
CC1=C(P(C2=CC=CC=C2)(C3=CC=CC=C3)=S)N4C(C=CC=C4)=[N+]1C/C=C/C5=CC=CC=C5.[Br-]

Molecular Weight: 545.47

Molecular Formula: C₂₉H₂₆N₂PS⁺ Br-ClogP: 2.73
H-Bond Donor: 0
H-Bond Acceptor: 1
Rotatable Bond Count: 6
Exact Mass: 544.07 (465.16 for cation)
Topological Polar Surface Area 41.1

Compound is soluble at 10 mM in DMSO. Solubility in PBS: Kinetic solubility >150 μ M, Thermodynamic solubility ~45 μ M.

Figure 2: The stability of CID 46930969 in PBS buffer for 120 h is illustrated in the graph below. The AUC at 254nm from a HPLC trace is plotted against time. No decomposition product was detected.



The probe CID 46930969 was analyzed in PBS buffer for stability. A 10 μ M DMSO (5 μ L) was diluted in PBS buffer (500 μ L) and the solution was analyzed by HPLC/MS. Two wavelengths (220 and 254 nm) were monitored. The normalized AUC for the probe compound at 254 nm is plotted against time (this data is presented above). We did not observe the formation of any other decomposition product during this analysis at either wavelength.

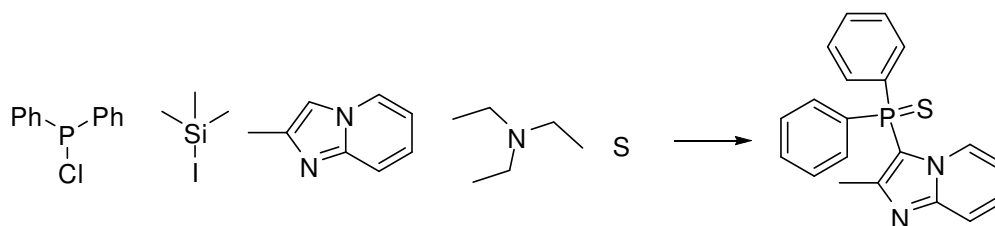
The hit compound CID 3278392 was analyzed in a similar way in Hanks' Balanced Buffer solution (HBSS; calcium chloride, magnesium chloride) for 48 h before medicinal chemistry optimization. HBSS is commonly used in biochemical assays. We did not detect the formation of any other species in that experiment as well.

2.3 Probe Preparation

General Methods: ¹H- and ¹³C NMR spectra were recorded on a Varian Inova 400 MHz spectrometer. Chemical shifts are reported in δ with the solvent resonance as the internal standard (DMSO-*d*₆ δ 2.50 for ¹H). Analytical analysis and retention times reported here were performed on an Agilent LC/MS (Agilent Technologies, Santa Clara, CA) with Method 1: A 7 minute gradient of 4 to 100% Acetonitrile (containing 0.025% trifluoroacetic acid) in water

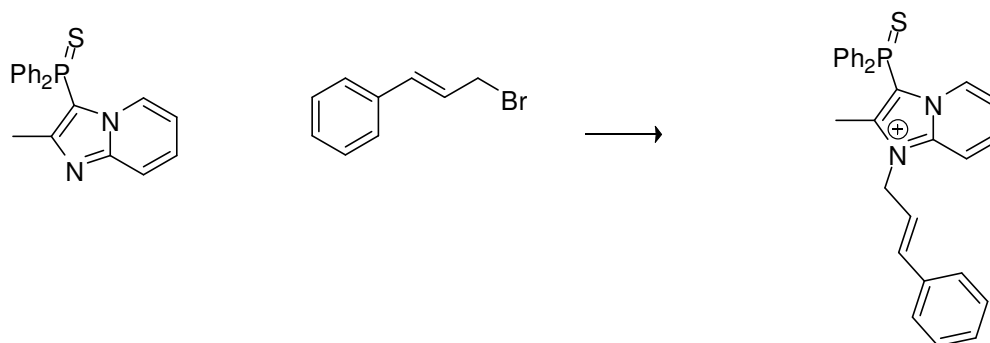
(containing 0.05% trifluoroacetic acid) was used with an 8 minute run time at a flow rate of 1 mL/min. A Phenomenex Luna C18 column (3 micron, 3 x 75 mm) was used at a temperature of 50 °C or Method 2: : A 3 minute gradient of 4 to 100% Acetonitrile (containing 0.025% trifluoroacetic acid) in water (containing 0.05% trifluoroacetic acid) was used with a 4.5 minute run time at a flow rate of 1 mL/min. A Phenomenex Gemini Phenyl column (3 micron, 3 x 100 mm) was used at a temperature of 50 °C. Confirmation of molecular formula was confirmed using electrospray ionization in the positive mode with the Agilent Masshunter software (version B.02). Molecular weight was confirmed using a TOF Mass Spectrometer (Agilent Technologies, Santa Clara, CA). A 3 minute gradient from 4 to 100% Acetonitrile (0.1% formic acid) in water (0.1% formic acid) was used with a 4 minute run time at a flow rate of 1 mL/min. A Zorbax SB-C18 column (3.5 micron, 2.1 x 30 mm) was used at a temperature of 50 °C. Confirmation of molecular formula was confirmed using electrospray ionization in the positive mode with the Agilent Masshunter software (version B.02).

3-(Diphenylphosphorothioyl)-2-methylimidazo[1,2-a]pyridine



Chlorodiphenylphosphine (3.89 ml, 26.4 mmol) and iodotrimethylsilane (5.29 g, 26.4 mmol) were stirred in toluene (10 ml) for 2 h. This was added to a premixed solution of 2-methylimidazo[1,2-a]pyridine (2.33 g, 17.6 mmol) and triethylamine (9.78 ml, 70.5 mmol) in pyridine (10.0 ml) and stirred 12 h. Sulfur powder (0.565 g, 17.6 mmol) was added and stirred for another 6 h. The reaction was concentrated, concentrated again with toluene (to remove pyridine), and diluted with benzene. The solids (presumed to be Et₃N and py salts) were filtered, and the filtrate, adsorbed over silica and subjected to purification by flash silica gel chromatography (0 to 75% EtOAc in DCM) to provide 3-(diphenylphosphorothioyl)-2-methylimidazo[1,2-a]pyridine (3.0 g, 8.7 mmol, 49 % yield). ¹H NMR (400 MHz, DMSO-*d*₆) δ ppm 1.57 (m, 3 H), 6.96 (m, *J*=6.7, 6.7, 1.0, 0.7 Hz, 1 H), 7.44 (m, 1 H), 7.60 (m, 4 H), 7.68 (m, 3 H), 7.78 (m, 4 H), 8.35 (dt, *J*=6.8, 1.2 Hz, 1 H); Method 1, retention time 2.97 min; HRMS (*m/z*) calcd for C₂₀H₁₈N₂PS⁺ (M+H)⁺ 349.0923, found 349.0927.

1-Cinnamyl-3-(diphenylphosphorothioyl)-2-methylimidazo[1,2-a]pyridin-1-ium, Br⁻



3-(Diphenylphosphorothioyl)-2-methylimidazo[1,2-a]pyridine and (E)-(3-bromoprop-1-enyl)benzene were reacted according to general procedure B to produce 1-cinnamyl-3-(diphenylphosphorothioyl)-2-methylimidazo[1,2-a]pyridin-1-ium, Br⁻. ¹H NMR (400 MHz, DMSO-*d*₆) δ ppm 1.75 (d, *J*=1.4 Hz, 3 H), 5.28 (m, 2 H), 6.43 (m, 1 H), 6.86 (d, *J*=16.0 Hz, 1 H), 7.32 (m, 3 H), 7.44 (m, 2H), 7.59 (td, *J*=7.1, 1.3 Hz, 1 H), 7.68 (m, 4 H), 7.78 (m, 2 H), 7.91 (m, 4 H), 8.20 (ddd, *J*=9.2, 7.2, 1.2 Hz, 1 H), 8.48 (m, 1 H), 8.70 (m, 1 H)); LC/MS: Method 1, retention time 3.27 min; Method 2, retention time 5.46 min; HRMS (*m/z*) calcd for C₂₉H₂₆N₂PS⁺ (M)⁺ 465.1549, found 453.1553.

2.4 Submission of samples to MLSMR

The following samples were submitted to the MLSMR repository:

MLS002703109 (probe)

MLS002703110

MLS002703111

MLS002703112

MLS002703113

MLS002703124

3 Results

The NIH Chemical Genomics Center specializes in developing high throughput assays to analyze compounds in the quantitative high throughput format (qHTS) to find probes towards biological pathways that have been implicated in various rare and neglected diseases.²¹ In an effort to discover antagonists for the NPS pathway, 220,874 compounds were screened using a cAMP-based IPOne assay.²² This endeavor led to the discovery of a NPS antagonist series with the capacity to antagonize, in a selective manner, the cAMP pathway or the calcium signaling pathways following NPS stimulation.¹⁹ From our screening, we also found the compound 3-(diphenylphosphorothioyl)-1,2-dimethylimidazo[1,2-a]pyridin-1-ium iodide **4** (Table 1, CID

16196125) having low micromolar activity ($IC_{50} \sim 1.12 \mu M$) in our cAMP assay.²³ Subsequently we ordered the powder and confirmed its activity. Our initial reservations about the unusual nature of the chemotype prompted us check the stability of the hit compound in Hank's balanced buffer, the buffer that was being used in our biological assays. We diluted a 10 mM DMSO solution of **4** with the buffer and stirred it for two days. We were pleased to find that neither *N*-demethylation nor conversion to the phosphorus oxide had taken place. The compound had maintained its integrity as evidenced by HPLC/MS. In addition to this, we did not observe any sign of cellular toxicity in our functional assays. Following these reassuring results, we decided to invest in further medicinal chemistry effort. Our initial goal was to develop a synthetic method toward the hit compound and analogs in order to establish the essential pharmacophore required for activity and then optimize for potency.

3.1 Summary of Screening Results

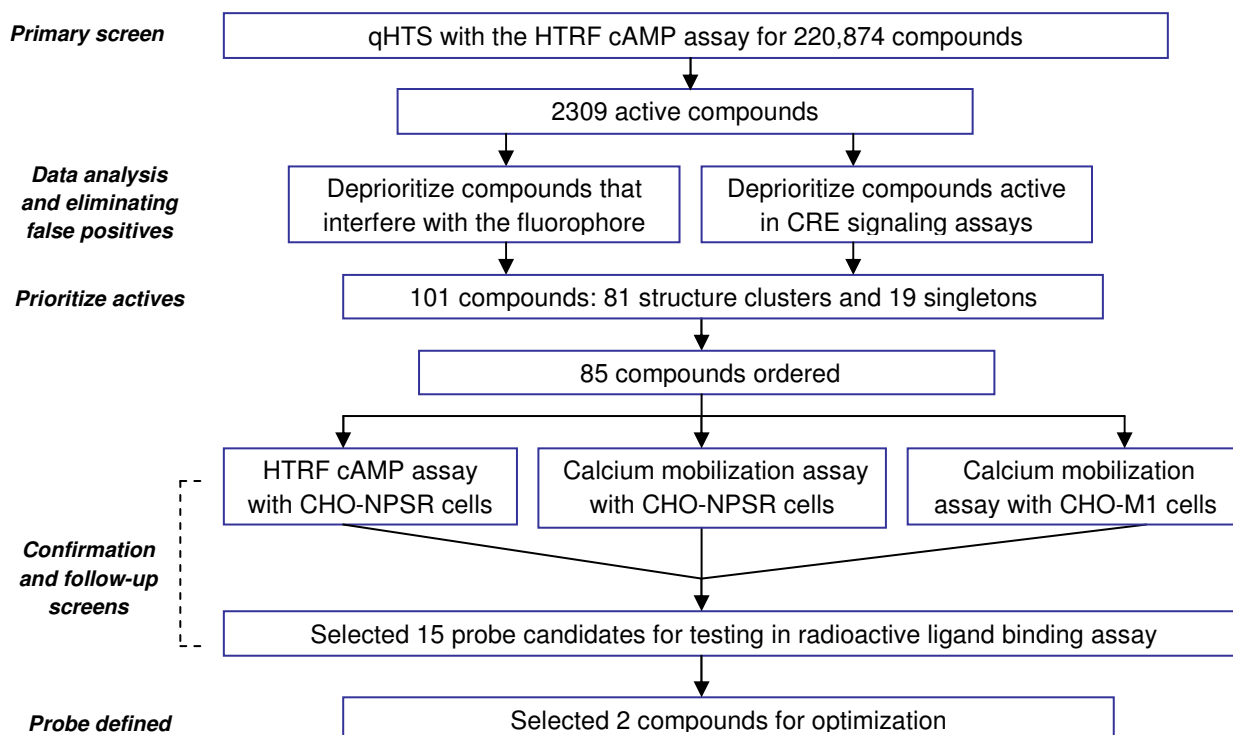


Figure 3: Overview of screening process.

NCGC tested 1284 1536-well plates in the primary screen (figure 3). The average Z' for the screen was 0.68 ± 0.10 , excluding 34 plates which failed visual QC. Results are reported for 221,370 samples. 2,309 compounds gave significant concentration-responses in the primary screen. Compounds were deprioritized for confirmation if they were suspected to interfere with the readout of the assay platform, or to affect GPCR signal transduction at a point in the

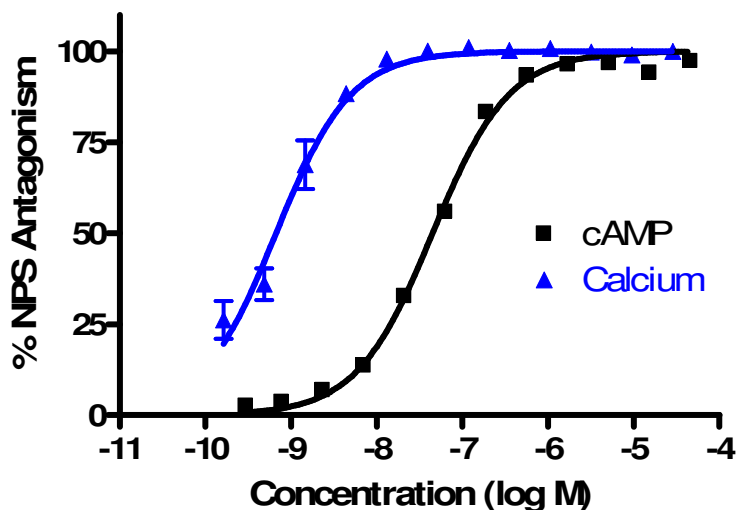
pathway beyond the neuropeptide S receptor using internal NCGC SAR data from other related assays.

Initially, only a portion of the MLPCN library was screened. This initial screening led to the discovery of MLS000558527 **3**, which had been disclosed as a probe. A later screening of compounds newly added to that library led to the discovery of MLS001018695 **4** as a screening hit. This novel chemotype prompted us to explore further the structure-activity relationship around the molecule, with the goal of further improving antagonist potency.

The activity of MLS001018695 **4** was subsequently confirmed by reordering the sample from the MLSMR, as well as the original supplier, Enamine (Catalog T0504-5950), confirming that sample for identity and purity using LC/MS (conditions given below), and then confirming activity in the primary screening assay examining antagonism of the cAMP response, as well as an assay for examining antagonism of NPSR's stimulation of intracellular calcium release.

3.2 Dose Response Curves for Probe

Figure 4: Concentration-response of the probe molecule, CID 46930969, in functional assays of NPSR antagonism: cAMP signaling IC₅₀ = 45nM (black) and calcium signaling IC₅₀ = 1nM (blue), 4 replicates each.



3.3 Scaffold/Moiety Chemical Liabilities

Active compounds from this chemical series, including the probe, have a phosphorothioyl moiety and N1-alkylated nitrogen in the imidazopyridine nucleus. The hit compound, as well as the probe, have been shown to be stable in Hank's buffer solution for 48 h and PBS for 120 h (this data is presented above) after incubation. No conversion to the phosphorus oxide or the dealkylated product is observed after 48 h in both buffers. Compounds from this chemical

series show activity in the cAMP and calcium functional assays in CHO-NPSR cells with no signs of toxicity. The hit and the probe show potent activity is a radiolabeled 125I-NPS displacement assay which does not monitor a fluorescence signal.

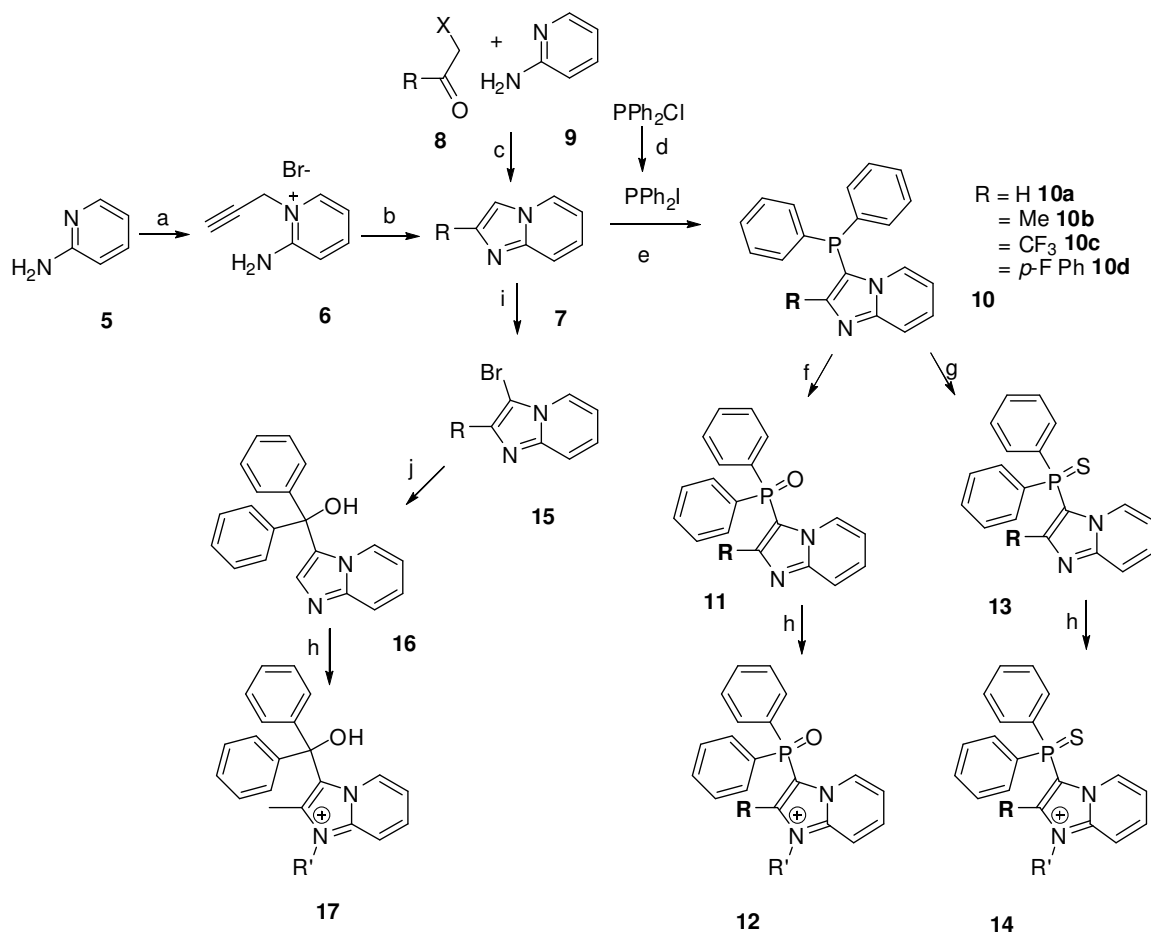
The probe molecule has a half life of 29.5 h in mouse liver microsomes. *In vivo* mouse PK experiments have indicated average concentrations of 1.5 μ M (0.08 h) to 0.05 μ M (24 h) of the parent ion with a 30 mpk IP dose. Mortality was observed at 12 h at this dose. A lower 10 mpk dose shows average plasma concentrations from 4.1 μ M (0.08 h) to 0.71 μ M (12 h) with no adverse events. This data is presented in detail later. Thus, although the probe and its congeners have a hitherto unknown drug-like structure, our studies have proven that they behave as stable and safe compounds in multiple *in vitro* as well *in vivo* experiments.

3.4 SAR Tables

Scheme 1 describes the chemistry route to the screening hit and its congeners. While the unsubstituted imidazo[1,2-*a*]pyridine **7a** was purchased from commercial sources, the 2-methylimidazo[1,2-*a*]pyridine **7b** was synthesized from 2-amino-1-(propargyl)pyridinium salt **6** via a palladium catalyzed cyclization.²⁴ Alternately α -haloketones **8** were condensed with 2-aminopyridine **9** to provide cores with different 2-substituted imidazopyridines **7c-d**.²⁵ Electrophilic aromatic substitution at the 3-position of the imidazopyridine ring by the diphenyl phosphino group was executed via the precedent of Tomalchev et al.²⁶ To that end, exposure to chlorodiphenylphosphine under basic conditions provided **10**, which could then be treated with elemental sulfur *in situ* to provide the phosphorothioyl species **13**. Treatment with hydrogen peroxide instead provided the corresponding phosphorus oxide **11**, an isosteric replacement for the phosphorothioyl species. Chlorodiphenyl phosphine proved to be unreactive towards 2-methylimidazopyridine, which could only be phosphorylated with the more reactive reagent iododiphenylphosphine.²⁷ The latter was generated from chlorodiphenyl phosphine and trimethylsilyliodide and was used without isolation.²⁸ The intermediates **11** and **13** could be then alkylated with various alkyl halides to generate compounds **12** and **14** for pharmacological analysis. A tertiary diphenyl alcohol group could also be a possible bioisostere for the phosphorothioyl group. The 3-bromo imidazopyridines **15** were generated by N-bromosuccinimide, towards that goal. Halogen-metal exchange using the chemistry described by Knochel was followed by addition of benzophenone to generate the tertiary alcohol **16**.²⁹ These alcohols could be chemoselectively alkylated the N-1 nitrogen in dioxane to yield final analogues **17**.

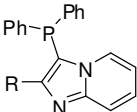
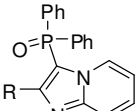
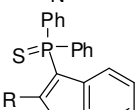
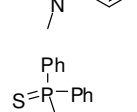
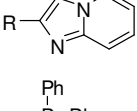
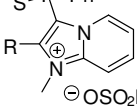
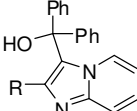
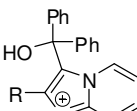
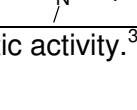




Compounds bearing an indole instead of the imidazopyridine were also synthesized in a similar manner to examine the importance of this nucleus in the pharmacophore. In this case, treatment with iododiphenylphosphine had to be followed by treatment with potassium hydroxide to break the N-P bond which had formed during the reaction.³⁰ The indole derivatives could then be alkylated as before. Tables 10 and 11 disclose the SAR of synthesized analogues.

Scheme 1^a: Synthetic methodology for the synthesis of initial lead **4** (CID 16196125) and analogues.

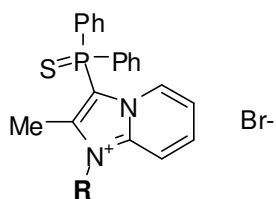


^aReagents and conditions. a) EtOH, $\text{CH}_3\text{CCH}_2\text{Br}$, reflux; b) $\text{Pd}(\text{PPh}_3)_4$, CuI, DMF, rt; c) EtOH, μwave , 150 °C; d) toluene; e) py, Et_3N ; f) 30% H_2O_2 ; g) sulfur; h) RBr, 1,4-dioxane, sealed tube, 100-120 °C; i) NBS, CH_2Cl_2 , -78 °C to rt; j) $i\text{-PrMgCl}$, THF, then Ph_2CO .

Table 10: SAR of initial analogues. The data presented here is an average of N=2

Comp#	CID	SID	Structure	R	cAMP IC ₅₀ (μM)	Ca ²⁺ IC ₅₀ (μM)
10a	44634514	87796311		H	inactive	35*
11a	44634519	87796307		H	inactive	inactive
11b	44634521	87796305		Me	inactive	inactive
18a	44634539	87796306		H	50*	inactive
18b	3989078	87796301		Me	32*	inactive
13a	44634544	87796302		H	50*	inactive
13b	44634570	87796303		Me	25*	17*
14a	44634578	87796299		H	32*	35*
4	3278392	87796297		Me	2.0	0.9
16a	44634533	87796309		H	inactive	inactive
16b	44634510	87796300		Me	79*	110*
17a	44634529	87796304		H	inactive	inactive
17b	44634524	87796310		Me	inactive	inactive

*These compounds disclosed partial antagonistic activity.³¹

Table 11: SAR of analogues in position one.

CID	SID	R	Cpd#	Ca ²⁺ IC ₅₀ (μM)	cAMP IC ₅₀ (μM)
3278392	87796298		4	0.050	1.7
44634561	87796317		19	0.032	1.3
44634508	87796315		20	0.073	2.1
44634569	87796313		21	0.080	2.1
44634512	87796316		22	0.002	0.11
46930969	87796314		23	0.001	0.05
46907767	99368032		24	0.001	0.94
46907769	99368034		25	0.013	0.71

3.5 Cellular Activity

The primary screening assay is a cell-based functional screening assay.

3.6 Profiling Assays

CID 46930969 was first profiled at 10 μ M against 8 other targets (Table 12). 90% activity was discovered in the mu-agonist displacement assay. IC50 determination by our collaborators in a radiolabeled displacement assay determined that the probe's activity against the mu-receptor was >500-fold less potent compared to the IC50 in the 125I-NPS displacement assay (Table 13 and figure 5).

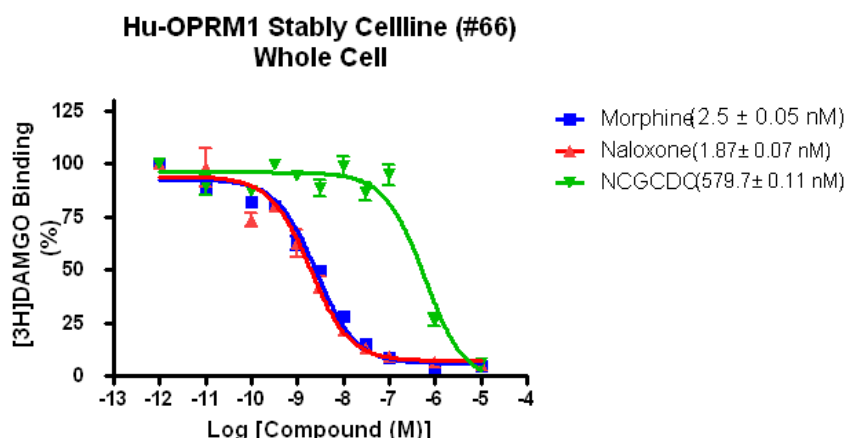
Table 12 The probe, CID 46930969, was profiled against 8 other targets at @ 10 μ M at Cerep®.

Assays	% of Control Agonist Response	Reference Compound
D1 (h) (agonist effect)	-0.4	dopamine
GABAB (h) (agonist effect)	1.3	3-APMPA
Y1 (h) (agonist effect)	-21.6	NPY
NTS1 (NT1) (h) (agonist effect)	-0.5	neurotensin
mu (MOP) (h) (agonist effect)	89.6	DAMGO
OX1 (h) (agonist effect)	-0.5	orexin-A
OT (h) (agonist effect)	-0.2	oxytocin
V1a (h) (agonist effect)	5.5	AVP

Table 13 CID 46930969 activity: NPSR vs. mu-opioid receptor (MOP)

Assay	IC50
NPS (displacement) Measure by our assay provider	1.0 nM
mu (MOP) (h) (displacement) Measured by Cerep	57 nM
mu (MOP) (h) (displacement) Measured by our assay provider	579 nM

Figure 5: CID 46930969 mu receptor activity (assay provider).



Subsequently, we profiled CID 46930969 at 10 μ M against 55 targets at Cerep® in binding assays. As a follow-up study, we determined IC₅₀s against targets which recorded >90% inhibition at 10 μ M. This data is presented in Table 14. This time we observed an IC₅₀ of 57 nM in the mu-agonist displacement assay at Cerep®. Although there is a 10-fold shift in potency between the MOP activities between Cerep and our assay provider, we have to be cognizant of this activity during *in vivo* studies.

Table 14: Profile of probe compound CID 46930969 in a full GPCR panel

CID 46930969 @ 10 μ M	
Assay	% Inhibition of Control Specific Binding
A1 (h) (antagonist radioligand)	18
A2A (h) (agonist radioligand)	32
A3 (h) (agonist radioligand)	27
alpha 1 (non-selective) (antagonist radioligand)	46
alpha 2 (non-selective) (antagonist radioligand)	14
beta 1 (h) (agonist radioligand)	17
beta 2 (h) (agonist radioligand)	6
AT1 (h) (antagonist radioligand)	-25
B2 (h) (agonist radioligand)	2
CB1 (h) (agonist radioligand)	69
CCK1 (CCKA) (h) (agonist radioligand)	25
D1 (h) (antagonist radioligand)	72
D2S (h) (antagonist radioligand)	83
ETA (h) (agonist radioligand)	6
GABA (non-selective) (agonist radioligand)	25
GAL2 (h) (agonist radioligand)	-24
CXCR2 (IL-8B) (h) (agonist radioligand)	-9
CCR1 (h) (agonist radioligand)	-13
H1 (h) (antagonist radioligand)	37
H2 (h) (antagonist radioligand)	23

MC4 (h) (agonist radioligand)	48
MT1 (ML1A) (h) (agonist radioligand)	57
M1 (h) (antagonist radioligand)	87
M2 (h) (antagonist radioligand)	IC50 = 0.59 μ M
M3 (h) (antagonist radioligand)	IC50 = 1.00 μ M
NK2 (h) (agonist radioligand)	1.5 μ M
NK3 (h) (antagonist radioligand)	15
Y1 (h) (agonist radioligand)	2
Y2 (h) (agonist radioligand)	41
NTS1 (NT1) (h) (agonist radioligand)	-1
delta 2 (DOP) (h) (agonist radioligand)	75
kappa (KOP) (agonist radioligand)	IC50 = 0.21 μ M
mu (MOP) (h) (agonist radioligand)	IC50 = 0.06 μ M
NOP (ORL1) (h) (agonist radioligand)	12
TP (h) (TXA2/PGH2) (antagonist radioligand)	-10
5-HT1A (h) (agonist radioligand)	77
5-HT1B (antagonist radioligand)	15
5-HT2A (h) (antagonist radioligand)	65
5-HT2B (h) (agonist radioligand)	6
5-HT3 (h) (antagonist radioligand)	21
5-HT5a (h) (agonist radioligand)	34
5-HT6 (h) (agonist radioligand)	20
5-HT7 (h) (agonist radioligand)	21
sst (non-selective) (agonist radioligand)	43
VPAC1 (VIP1) (h) (agonist radioligand)	-12
V1a (h) (agonist radioligand)	12
Ca ²⁺ channel (L, verapamil site) (phenylalkylamine) (antagonist radioligand)	83
KV channel (antagonist radioligand)	55
SKCa channel (antagonist radioligand)	-5
Na ⁺ channel (site 2) (antagonist radioligand)	IC50 = 0.2 μ M
Cl ⁻ channel (GABA-gated) (antagonist radioligand)	32
norepinephrine transporter (h) (antagonist radioligand)	86
dopamine transporter (h) (antagonist radioligand)	IC50 = 2.9 μ M
5-HT transporter (h) (antagonist radioligand)	75

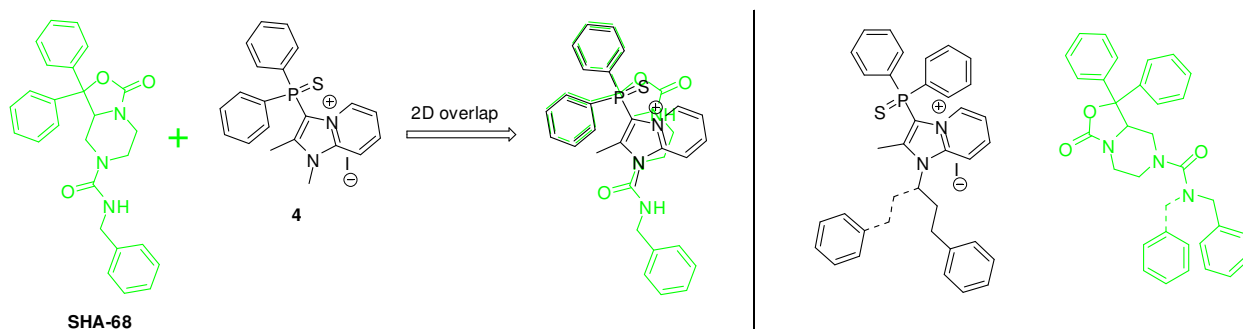
4 Discussion

Screening efforts at NCGC led to the discovery of phosphorothioyl 4 as a hit against NPSR. The antagonistic properties of the screening hit were reconfirmed with purchased powder and established in two functional assays, as well as a ¹²⁵I NPS displacement assay. The chemotype possessed a rather unusual structure, with a diphenylphosphorothioyl species and an alkylated N1 imidazopyridine core. Our initial assessment of stability in aqueous buffer obviated concerns regarding potential decomposition pathways involving demethylation or conversion to the phosphorus oxide species. Subsequently, we developed a robust chemistry route to the hit and analogs (Scheme 1). The antagonistic potencies of synthesized compounds were then

evaluated in two functional assays where IC_{50} s were calculated for the inhibition of increase of calcium or cAMP concentrations on addition of NPS to CHO cells permanently expressing NPSR. The resynthesized hit **4** confirmed the activity of the original screening hit. However, the initial SAR revealed that there was very little room for modifying the parent structure of the hit (Table 4). Thus, the synthetic phosphine precursor **10a**, without the sulfur and the methyl substituent at position one, was inactive. Analogues without the methyl substitution at position two, compounds **11a**, **18a**, **13a**, **14a**, **16a** and **17a**, disclosed no activity, or a huge reduction in efficacy and IC_{50} . Moreover, reintroduction of methyl group in two position of the indole series, **18b** derivative, was not enough to restore the potency and resulted in compounds with partial efficacy curves.³⁰ The examination of possible bioisosteric replacements of the phosphorothioyl moiety proved futile, as the phosphorus oxide **11b** and the diphenyl tertiary alcohols **16b** and **17b** had hardly any measurable activity in the functional assays.

A careful examination of the chemical structure of SHA66/68 and our screening hit prompted us to evaluate two and three dimensional overlap models, Figure 6. In house 125I-NPS displacement experiments disclosed that both series are able to compete with the natural ligand, and therefore, we hypothesized that both orthosteric antagonists should bind in the same region, probably with similar three dimensional geometry. An alignment of the gem-diphenyl groups in both chemotypes indicated that our lead compound **4** probably lacked a benzylic hydrophobic moiety, present in SHA68. This motif has been shown to be fundamental in providing analogues with high potency, and was able to further enhance the binding with the receptor. To that end, the 1-nitrogen of the imidazopyridine provided a convenient point of divergence for alkylation with a variety of commercially available alkyl bromides. The idea was to synthesize analogues with a phenyl group at different spacer units from the imidazopyridine nucleus.

Figure 6: Two dimensional overlap of SHA-68 and lead compound **4**.



As enumerated in Table 5, the strategy to explore a hydrophobic pocket a few atoms away from the N-1 imidazopyridine nucleus proved to be a fruitful exercise. Compounds with a phenyl unit one (**19**) or two carbon atoms (**20**) had similar potencies as the original hit, although the phenyl ethanone **21** lost 1-2 fold potency in the cAMP and calcium assays. Remarkably, the compound with the phenyl propyl chain **22** recorded substantial improvements in potency with 250 nM IC_{50} in the cAMP assay and 40 nM IC_{50} in calcium assays. The same trend was observed for the more constrained propenylbenzene appendage **23**. Thus, it seemed that a hydrophobic pocket in the enzyme was making a favorable contact with a phenyl group which was three atoms away

from the N-1 nitrogen. An extension by one or two more carbons led to a drop in potency, as evidenced by the cAMP IC₅₀s in **24** and **25**. Interestingly, an application of the same SAR strategy on the indole replacement for the imidazopyridine core did not resurrect the potency implying the importance of this nucleus for activity.

In our hands, compound **23** (CID 46930969) showed slightly better activity than quinolinone **2a** disclosed by Merck (Table 19 below). We observed a >40-fold and >100-fold improvement in the cAMP and calcium assay IC₅₀ compared to SHA68. We wanted to evaluate further if the chemotype discovered by us offered advantages over the existing NPSR antagonists. Figure 7 compares the calculated log and total polar surface area values for the three most active small molecule NPS antagonists known to date. All of the calculated values for the three series were promising for CNS penetration. Next, we examined the stability of these compounds in mouse liver microsomes with NADPH, the required co-factor for p450 mediated oxidation, at 15, 30 and 60 min. It can be seen from Table 15 that although our probe possesses an unusual structure, the microsome stability is much superior with half life of 29.5 h. This bodes well for planned *in vivo* studies. In addition to this clear advantage and in contrast to the other series, our probe does not bear a chiral center.

Figure 7: Comparison of physical properties of previously disclosed small molecule NPS antagonists. Properties computed using ChemDraw 12.0.

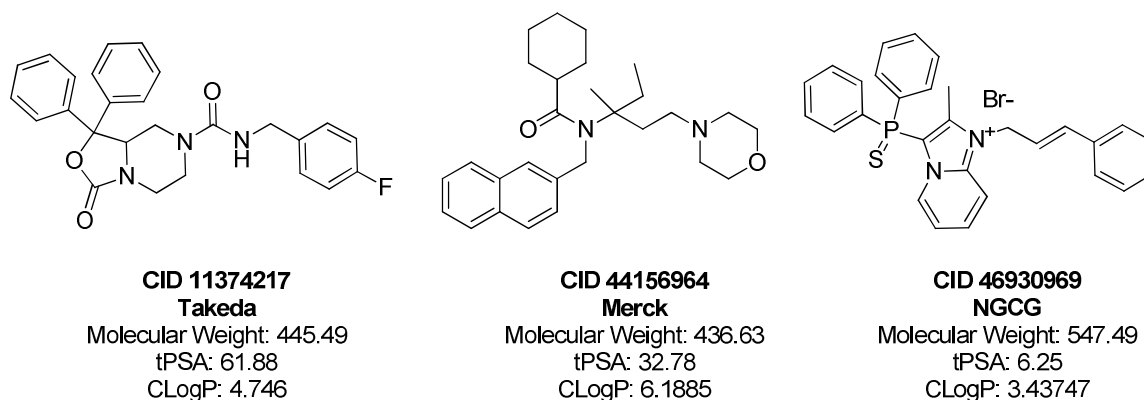
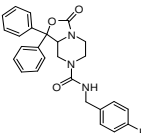
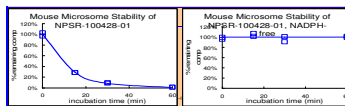
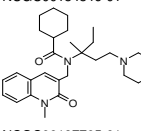
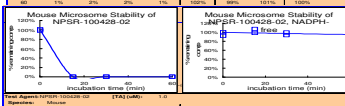
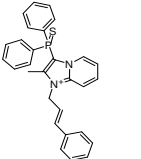
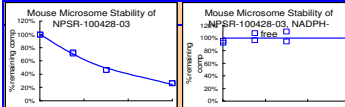


Table 15: Comparison of the microsomal stability of all top three NPSR antagonists

Client ID	conc (μM)	species	NADPH-dependent	NADPH-dependent	NADPH-free	NADPH-free	M+			
			CL _{int} ^a	T _{1/2} ^b	CL _{int} ^a	T _{1/2} ^b				
			(μ min ⁻¹ mg ⁻¹)	(min)	(μ min ⁻¹ mg ⁻¹)	(min)				
Verapamil	1	Mouse	752.1	<3.3	0	<3.3				
Warfarin	1	Mouse	4.3	>180	0	<3.3				
	SHA68	NCGC00184846-01	1	Mouse	273.5	8.4	0	<3.3	445	
	Merck	NCGC00187765-01	1	Mouse	1739.3	<3.3	0	<3.3	467	
	NCGC	NCGC00185684-01	1	Mouse	78.3	29.5	0	<3.3	465	

<

^aMicrosomal Intrinsic Clearance
^bHalf-life

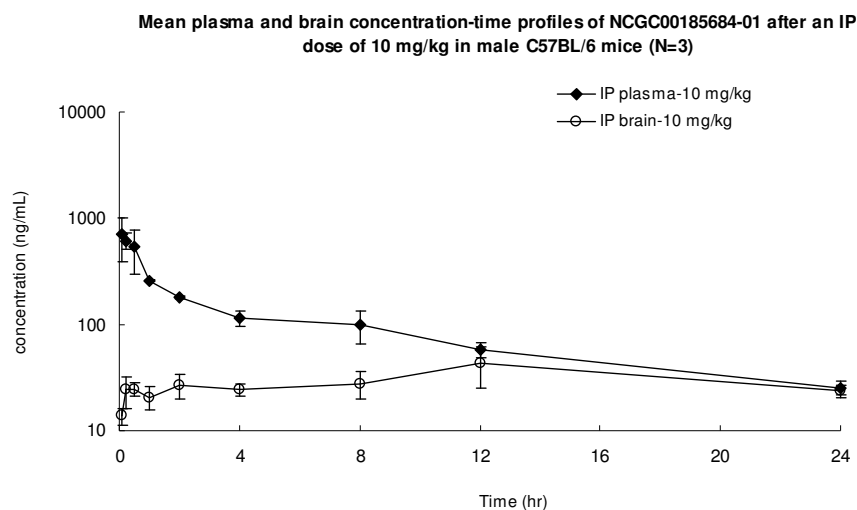
The stability in mouse liver microsomes spurred an evaluation of the pharmacokinetics of CID 46930969 in order to plan the correct doses for *in vivo* studies. Tables 16 and 17 describe the PK of the probe molecule at a 10 mpk doses in mice. Gratifyingly, there were no signs of adverse effects with this dose. The mice appeared healthy with compound concentrations ranging from 1.5 to 0.05 μM in the plasma and 30 to 93 nM in the brain. Significantly, the compound concentration in the brain was still above the *in vitro* IC₅₀ at 24h. By comparison, the reported *in vivo* rat PK of quinolinone **2a** from Merck at 30 mg/kg IP dose reveals the following tissue levels at 0.5 h: Plasma/Brain/CSF (nM) = 4344, 1690, 101 and at 2.0 h: Plasma/Brain/CSF (nM) = 2297, 665, 45. SHA68 (**1b**) reaches the following concentrations in mice after a 50 mpk IP dose at 15 min: Plasma/Brain, 88, 6.3 μM and at 2.0 h: 1.1, 2.1 μM. Thus, these two compounds appear to be rapidly cleared from the plasma and the brain, and this is consistent with the *in vitro* microsomal stability data generated by NCGC. Our probe, CID 46930969, seems to maintain steady concentrations well above the IC₅₀ for 24 h when it is administrated IP at a dose of 10 mg/kg. This may be critical for *in vivo* activity, as SHA68 only shows partial efficacy in a hyperlocomotion mouse model. With the lack of *in vivo* efficacy animal data in disease models with the other potent NPSR antagonists **2a/2b/3**, we feel that the relevance of the NPS/NPSR neurocircuitry towards disease states is still unexplored. At this stage, we decided to examine our most characterized probe compound **23** in an animal model where hyperactivation of the NPS signaling causes a suppression of food intake in rodents.³² Thus, with *in vivo* administration of our probe, CID 46930969, we expected a reversal in the food intake suppression.

Table 16: CID 46930969 Mouse Pharmacokinetics: Concentrations in Plasma and Brain of Probe at 10 mpk IP dose

Sampling time(hr)	10 mpk			
	Plasma		Brain	
	Mean (ng/mL)	Mean nM	Mean (ng/mL)	Mean nM
0	BQL	BQL	BQL	BQL
0.083	700	1503	14	30
0.25	617	1325	24	52
0.5	536	1150	25	53
1	259	556	21	44
2	180	386	27	57
4	114	245	24	53
8	99	214	28	60
12	58	126	43	93
24	25	54	24	52

Table 17: CID 46930969 Mouse PK Paramaters and Curve for 10 mpk IP dose

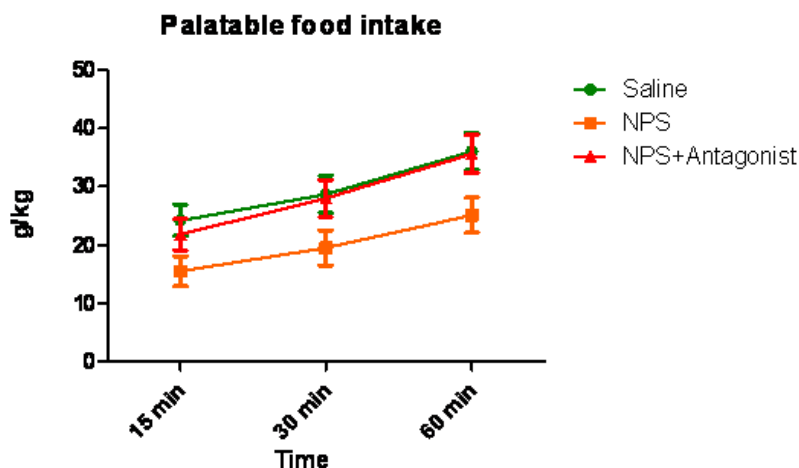
PK parameters	Unit	Estimate	PK parameters	Estimate
Tmax	hr	0.083	Tmax	12
Cmax	ng/mL	700	Cmax	43
T1/2	hr	8.8	T1/2	N/A
AUCplasma(AUClast)	hr*ng/mL	2240	AUCbrain(AUClast)	746
AUCINF	hr*ng/mL	2560	AUCINF	N/A
AUCbrain/AUCplasma	%	33		



In our preliminary *in vivo* experiment, rats with intracranial implants were habituated to a sweetened diet. The food intake was measured at 15, 30, and 60 min in a control group and in animals where NPS was administered icv (Figure 8). Animals were balanced between groups so that the pre-test baseline intake was matched. The NPS induced reduction in food intake

(orange line) compared to controls (green) was completely reversed by intracerebroventricular (icv) administering of the antagonist **23** (10 μ g) prior to NPS administration (6-8 animals/group).

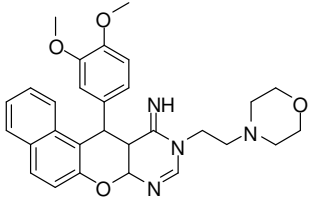
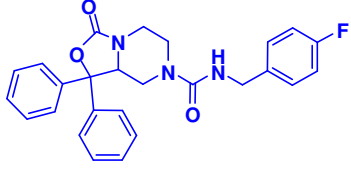
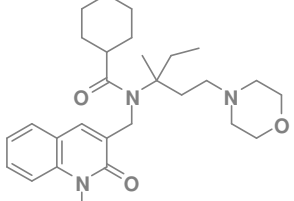
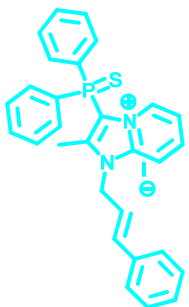
Figure 8: CID 46930969 Food Intake icv Experiment

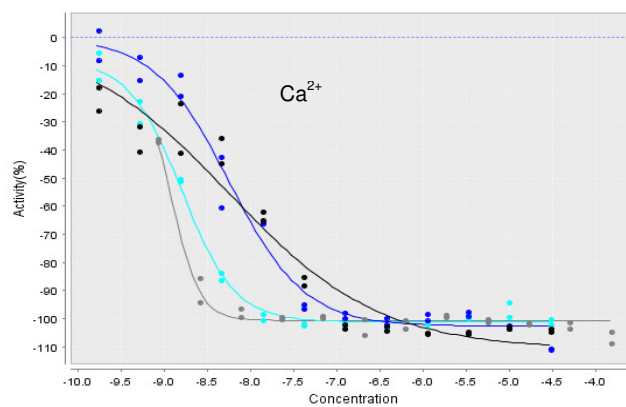
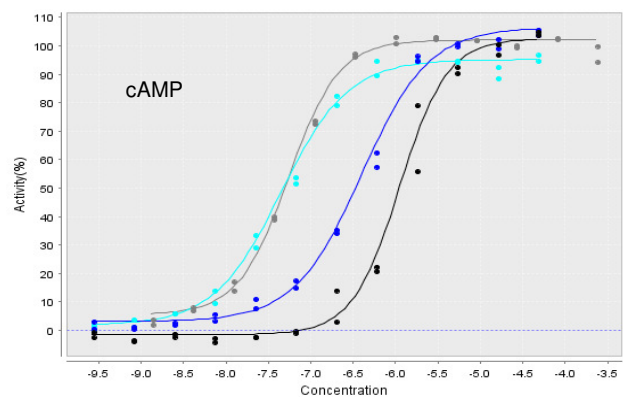


4.1 Comparison to existing art and how the new probe is an improvement

In summary, the qHTS paradigm at NCGC was used to identify a structurally novel small molecule as an antagonist for the study of NPS-NPSR neurocircuitry. Further medicinal chemistry revealed the uniqueness of this chemotype towards receptor binding, in that even slight modifications to the structure lead to a dramatic loss of activity. Simple overlap models with a previously disclosed inhibitor prompted a SAR study, which led to the synthesis of the potent analogs **22** and **23**. The latter was characterized as a potent antagonistic in functional and binding assays. The unique nature of the chemotype also promoted stability studies, which proved that the compounds were stable in buffer despite their unusual structure. The probe also had remarkable stability in mouse liver microsomes which was substantiated via *in vivo* PK experiments. A 10 mpk IP dose secured micromolar levels in the plasma with slow clearance. The compound maintained levels in the brain above the *in vitro* IC₅₀ against NPSR through the last time point of measurement (24h). Finally, icv administration of the antagonist completely reversed NPS-induced suppression of food intake in rats. Thus, our probe represents the first small molecule which shows complete efficacy in a NPS-mediated *in vivo* disease model. The PK studies delineate why slow clearance with **23** might provide us unique advantages over the existing compounds.

Table 19: Comparison of activity between reported NPS antagonists

Cpd#	Comments	Structure	¹²⁵ I-hNPS displacement IC ₅₀ nM	Ca ²⁺ IC ₅₀ nM	cAMP IC ₅₀ nM
MLS000558527	First NCGC probe		190	1585	1259
NCGC00184846	SHA68		5.9	139	1940
NCGC00187765	Merck Lead		6.5	1	55
CID 46930969	Second NCGC probe		1	1	45



4.2 Mechanism of Action Studies

N/A

4.3 Planned Future Studies

5 References

¹ Holmes, A.; Heilig, M.; Rupniak, N. M. J.; Steckler, T.; Griebel, G. *Trends in Pharmacological Sciences* **2003**, *24*, 580-588.

² Sato, S. S. Y.; Miyajima, N.; Yoshimura, K. Novel G-protein coupled receptor protein and DNA thereof, *World Patent Application WO 02/31145 A1*. **2002**.

³ Xu, Y. L.; Reinscheid, R. K.; Huitron-Resendiz, S.; Clark, S. D.; Wang, Z.; Lin, S. H.; Brucher, F. A.; Zeng, J.; Ly, N. K.; Henriksen, S. J.; de Lecea, L.; Civelli, O. *Neuron* **2004**, *43*, 487– 497.

⁴ Y.L. Xu, C.M. Gall, V.R. Jackson, O. Civelli and R.K. Reinscheid, Distribution of neuropeptide S receptor mRNA and neurochemical characteristics of neuropeptide S-expressing neurons in the rat brain, *Journal of Comparative Neurology* **500** (2007), pp. 84–102.

⁵ For reviews on the NPS/NPSR pathway see: (a) Pape, H.; Juengling, K.; Seidenbecher, T.; Lesting, J.; Reinscheid, R. K. *Neuropharmacology* **2009**, *58*, 29-34. (b) Okamura, N.; Reinscheid, R. K. *Stress*, **2007**, *10*, 221-226. (c) Lei, Z.; Yao, Y. Li, Y. Yang, G. *Xumu Yu Shouyi* **2008**, *40*, 97-100.

⁶ Laitinen, T.; Polvi, A.; Rydman, P.; Vendelin, J.; Pulkkinen, V.; Salmikangas, P.; Makela, S.; Rehn, M.; Pirskanen, A.; Rautanen, A. et al. *Science*, **2004**, *304*, 300-304.

⁷ Reinscheid, R. K.; Xu, Y. L.; Okamura, N.; Zeng, J.; Chung, S.; Pai, R.; Wang, Z.; Civelli, O. *J. Pharmacol. Exp. Ther.* **2005**, *315*, 1338– 1345.

⁸ Clark, S. D.; Tran, H. T.; Zeng, J.; Reinscheid, R. K. *Peptides* **2010**, *31*, 130-138

⁹ Castro, A. A.; Moretti, M.; Casagrande, T. S.; Martinello, C.; Petronilho, F.; Steckert, A. V.; Guerrini, R.; Calo', G.; Dal Pizzol, F.; Quevedo, J.; Gavioli, E.C. *Pharmacology, Biochemistry and Behavior* **2009**, *91*, 636–642.

¹⁰ Beck, B.; Pourie, C.; Gueant, J. *Psychopharmacology* **2008**, *197*, 601-611.

¹¹ Cannella, N.; Economidou, D.; Kallupi, M.; Stopponi, S.; Heilig, M.; Massi, M.; Ciccocioppo, R. *Neuropsychopharmacology* **2009**, *34*, 2125-2134.

- ¹² (a) Paneda, C.; Huitron-Resendiz, S.; Frago, L. M.; Chowen, J. A.; Picetti, R.; de Lecea, L.; Roberts, A. J. *Journal of Neuroscience* **2009**, 29, 4155-4161. (b) Li, W.; Gao, Y.; Chang, M.; Peng, Y.; Yao, J.; Han, R.; Wang, R. *Peptides* **2009**, 30, 234-240.
- ¹³ Reinscheid, R. K. *Peptides* **2007**, 28, 830-837.
- ¹⁴ (a) Guerrini, R.; Camarda, V.; Trapella, C.; Calo, G.; Rizzi, A.; Ruzza, C.; Fiorini, S.; Marzola, E.; Reinscheid, R. K.; Regoli, D.; Salvadori, S. *J. Med. Chem.* **2009**, 52, 4068-4071; (b) Guerrini, R.; Camarda, V.; Trapella, C.; Calo, G.; Rizzi, A.; Ruzza, C.; Fiorini, S.; Marzola, E.; Reinscheid, R. K.; Regoli, D.; Salvadori, S. *J. Med. Chem.* **2009**, 52, 524-529; (c) Camarda, V.; Trapella, C.; Calo, G.; Guerrini, R.; Rizzi, A.; Ruzza, C.; Fiorini, S.; Marzola, E.; Reinscheid, R. K.; Regoli, D.; Salvadori, S. *J. Med. Chem.*, **2008**, 51, 655-658.
- ¹⁵ Fukatsu, K.; Nakayama, Y.; Tarui, N.; Mori, M.; Matsumoto, H.; Kurasawa, O.; Banno, H. *PCT Int. Appl.* **2005**, WO 2005021555 A1 20050310
- ¹⁶ Okamura, N.; Habay, S. A.; Zeng, J.; Chamberlin, A. R.; Reinscheid, R. K. *Journal of pharmacology and experimental therapeutics* **2008**, 325, 893-901.
- ¹⁷ Melamed, J. Y.; Zartman, A. E.; Kett, N. R.; Gotter, A. L.; Uebele, V. N.; Reiss, D. R.; Condra, C. L.; Fandozzi, C.; Lubbers, L. S.; Rowe, B. A.; McGaughey, G. B.; Henault, M.; Stocco, R.; Renger, J. J.; Hartman, G. D.; Bilodeau, M. T.; Trotter, B. W. *Bioorg. Med.Chem.Lett.* **2010**, 20, 4700-4703.
- ¹⁸ Trotter, B. W.; Nanda, K. K.; Manley, P. J.; Uebele, V. N.; Condra, C. L.; Gotter, A. L.; Menzel, K.; Henault, M.; Stocco, R.; Renger, J. J.; Hartman, G. D.; Bilodeau, M. T. *Bioorg. Med.Chem.Lett.* **2010**, 20, 4704-4708.
- ¹⁹ McCoy, J. G.; Marugan, J. J.; Liu, K.; Zheng, W.; Southall, N.; Heilig, M.; Austin, C. A. *ACS Chem. Neurosci.* **2010**, 1, 559-574.
- ²⁰ Xu, Y.L., Reinscheid, R.K., Huitron-Resendiz, S., Clark, S.D., Wang, Z., Lin, S.H., Brucher, F.A., Zeng, J., Ly, N.K., Henriksen, S.J., de Lecea, L., Civelli, O. *Neuron* **2004**, 43 (4), 487-97
- ²¹ <http://www.ncgc.nih.gov/>
- ²² Liu, K.; Titus, S.; Southall, N.; Zhu, P.; Inglese, J.; Austin, C. P.; Zheng, W. *Current Chemical Genomics* **2008**, 1, 70-78.
- ²³ Available commercially at Enamine, Cat# T0504-5950.
- ²⁴ Bakherad, M.; Nasr-Isfahani, H.; Keivanloo, A.; Doostmohammadi, N. *Tetrahedron Letters* **2008**, 49, 3819-3822.
- ²⁵ For a similar recent procedure see Tong, Y. et al. *J. Med. Chem.* **2009**, 52, 6803-6813.
- ²⁶ Tomalchev, A. A.; Yurchenko, A. A.; Kozlov, E. S.; Merkulov, A. S.; Semenova, M. G.; Pinchuk, A. M. *Heteroatom Chemistry* **1995**, 5, 419-432.

- ²⁷ Tomalchev, A. A.; Yurchenko, A.A.; Kozlov, E.S. *J. Gen. Chem. USSR (Engl. Transl.)* **1992**, 62, 1369-1371.
- ²⁸ Romanenko, V. D.; Tovstenko, V. I.; Markovski, L. N. *Synthesis* **1980**, 10, 823-825.
- ²⁹ Krasovskiy, A.; Knochel, P. *Angew. Chem. Int. Ed.* **2003**, 43,3333-3336.
- ³⁰ Benincori, T.; Piccolo, O.; Rizzo, S.; Sannicolò, F. *J. Org. Chem.* **2000**, 65, 8340-8347.
- ³¹ <http://www.pnas.org/content/suppl/2009/02/05/0813020106.DCSupplemental/0813020106SI.pdf>
- ³² Fedeli, A.; Braconi, S.; Economidou, D.; Cannella, N.; Kallupi, M.; Guerrini, R.; Calò, G.; Cifani, C.; Massi, M.; Ciccocioppo, R. *Eur. J. Neurosci.* **2009**, 30, 1594-1602.
- ^{33 33} Badia-Elder, N. E., Henderson, A. N., Bertholomey, M. L., Dodge, N. C., Stewart, R. B. *Alcohol Clin. Exp. Res.* **2008**, 32, 1380-1387.
- ³⁴ Ciccocioppo, R. Heilig, M., et al. *Neuropsychopharm.* **2009**, 34, 2125-2134.